Available online at www.sciencedirect.com
SCIENCE DIRECT®
International Journal of Heat and Mass Transfer 47 (2004) 3549–3563
International Journal of HEAT and MASS TRANSFER
www.elsevier.com/locate/ijhmt

Natural convection in rectangular tanks heated locally from below

I.E. Sarris, I. Lekakis, N.S. Vlachos *

Department of Mechanical and Industrial Engineering, University of Thessaly, Athens Avenue, 38334 Volos, Greece

Received 25 March 2003; received in revised form 4 December 2003

Abstract

The present study was undertaken in order to gain understanding of certain aspects of natural convection in a glass-melting tank heated locally from below. Based on numerical predictions, the effects of Rayleigh number, geometry of heated strip and tank on the flow patterns and heat transfer are investigated for Rayleigh numbers in the range 10^2 to 10^7, strip width to tank length ratios 0.1–0.5 and half-tank aspect ratios 1.0, 3.0 and 7.0. The effect of the heated strip position is studied by placing it at centre and off-centre positions at the tank bottom wall. The effect of Rayleigh number on heat transfer is found to be significant. The Nusselt number is obtained as a function of Rayleigh number, heated strip width to tank length ratio and tank aspect ratio. Augmentation of flow circulation intensity and fluid temperature results when increasing the tank length and strip width. A scale analysis led to a behaviour which is confirmed by the numerical results.

1. Introduction

Natural convection above horizontal heated surfaces appears in a variety of physical circumstances (e.g. thermal plumes, meteorological and geophysical phenomena) as well as in industrial equipment (e.g. cooling of electronics, veneer). The melting of glass is another important industrial application in which horizontal heated surfaces could play a significant role. Motivated by the glass melting process, the present numerical study examines in detail the important parameters of the natural convection above heated horizontal surfaces located on the bottom wall of open enclosures such as those of glass melting tanks.

Although several studies have been performed on the natural convection along vertical plates, a very limited number of studies examine the problem of natural convection heat transfer above a horizontal plate. The heat transfer in a vertical cylindrical enclosure subjected to localized heating at the centre of its bottom wall was studied numerically by Torrance and Rockett [1] and experimentally by Torrance et al. [2]. Their numerical and experimental results show very good agreement in the laminar flow regime. Pretot et al. [3] reported a numerical and experimental study of natural convection in air above an upward-facing partially heated plate placed in a semi-infinite medium. Sezai and Mohamad [4] also studied numerically natural convection in air due to a discrete flush-mounted rectangular heat source on the bottom of a horizontal enclosure. Boehm and Kamyab [5] studied laminar natural convection of air, due to stripwise heating accomplished by an array of alternatively heated and non-heated strips placed on an infinite horizontal surface in a fluid of infinite extent. Chu and Hickox [6] studied localized heating from below in a horizontal enclosure of square platform which contained a temperature-dependent property fluid. In their work, which was complemented by experiments, a constant-temperature heated strip of fixed width was placed on the bottom wall of the enclosure. Aydin and Yang [7] simulated numerically the natural convection heat transfer of air in a two-dimensional, square enclosure with localized heating applied by a strip placed at the

* Corresponding author.
E-mail address: vlachos@mie.uth.gr (N.S. Vlachos).

0017-9310/$ - see front matter © 2004 Elsevier Ltd. All rights reserved.
doi:10.1016/j.ijheatmasstransfer.2003.12.022

Nomenclature

A	aspect ratio of half-tank, L/H
A_s	heated strip ratio, W_s/L
g	gravitational acceleration
H	tank height
k	thermal conductivity
L	tank half length
L_t	tank total length ($=2L$)
Nu_{fs}	local Nusselt number at the free surface
$\overline{Nu}$	average Nusselt number at the heated strip
p	fluid pressure
P	dimensionless pressure
Pr	Prandtl number
q''	heat flux rate from the strip
Ra	Rayleigh number
T	fluid temperature
t	time
u, v	velocity components in x and y directions
U, V	dimensionless velocity components
x, y	spatial coordinates
X, Y	dimensionless coordinates
W_s	strip width

Greek symbols

α	thermal diffusivity
β	coefficient of thermal expansion
Θ	non-dimensional temperature
ν	fluid kinematic viscosity
ρ	fluid density
τ	non-dimensional time
ϕ	generalized variable
Ψ	non-dimensional stream function

Subscripts

fs	free surface
s	strip
t	total
max	maximum
i, j	coordinate indices
0	reference value

bottom wall centre and symmetric cooling from the side walls. Their analysis included the influence of the heated strip width and Rayleigh number on the fluid flow and heat transfer. Katsavos et al. [8] studied experimentally and numerically the natural convection of a temperature-dependent fluid above a heated wire placed on the bottom of a rectangular tank with the use of an in-house PIV system. Emery and Lee [9] studied the effect of property variations on the natural convection in a square enclosure with different boundary conditions on the sidewalls. A comparison of the results for a variable property fluid with those of a constant property showed that, although the fluid flow and temperature fields seem to be different, the overall heat transfer is unaffected by the variation of the fluid properties.

The idea of using heated strips in glass-melting tanks seems to originate from Plumat [10]. He employed heated strips placed at the bottom of the tank and normal to its main axis in physical model studies in order to enhance the melting procedure. The effect of horizontal heated strips at the bottom wall of an industrial glass melting tank in two- and three-dimensions was studied numerically by Sarris et al. [11]. Increasing the average temperature of the glass-melt, especially in the region above the cold bottom wall is of great practical importance to the glass industry.

The heating of glass-melting tanks is mainly implemented through radiation from the flames and the combustion chamber just above the tank. As a consequence, the free surface temperature is controlled by the radiation absorption of glass-melt. Cheong et al. [12] showed that the Rosseland (or diffusion) approximation is adequate to account for the radiation heat transfer in industrial glass-melting tanks. This is achieved through the concept of the effective thermal conductivity. The natural convection due to the temperature variations at the free surface is usually the driving force for the whole flow of the glass-melt, considering the very low pulling rates of the raw materials. Extensive discussions on the effects of the free surface temperature distribution on the flow and heat transfer of the glass-melt can be found, among others, in [13]. Modern glass-heating furnaces include a large number of closely spaced burners, resulting in almost uniform temperature distribution at the glass-melt free surface and in considerable reduction of mixing. Therefore, in order to enhance mixing, electric boosting and/or air bubbles are usually introduced into the melt. The alternative method of using heated strips at the bottom wall, which has the advantage of enhancing localized mixing at the places where it is needed most, has not been considered in the open literature. The results presented here show for which working parameters this method can be effective.

In the present work, the natural convection in a rectangular tank heated with a strip placed at the bottom wall of the tank is studied numerically, using a fluid with the same temperature-dependent properties as the glass-melt. The objective is to determine the influence of the heated strip on the flow and heat transfer characteristics of the glass-melt under uniform free surface

temperature distribution and to optimize the strip dimensions and heating conditions for efficient mixing of the melt.

2. Mathematical formulation

Consider a rectangular open tank of length $L_t = 2L$ with a heated strip of width $2W_s$ at the bottom of the tank, as shown in Fig. 1, and filled up to height H with glass melt. The boundary conditions considered are: no-slip on the solid boundaries, zero shear stress and zero vertical velocity at the free surface. The temperature of the free surface is kept constant and the tank walls are considered adiabatic while a uniform heat lux q'' is assumed for the heated strip.

The glass-melt is considered as Newtonian fluid, and the flow incompressible and laminar. For the treatment of the buoyant term in the momentum equation, the extended Oberbeck [14]–Boussinesq [15] approximation is adopted, to account for the temperature variations of density, viscosity and thermal conductivity. Hofmann [16] provides a detailed discussion on the validity of the extended Boussinesq approximation as applied to the simulation of glass melt in industrial tanks. The specific heat and the coefficient of thermal expansion of the glass melt are considered temperature independent in the high-temperature ranges of the melt, Jian and Zhihao [17]. The thermo-physical properties of the glass-melt used are shown in Table 1. Based on these assumptions, the governing equations in dimensionless form for a two-dimensional flow become

$$\frac{\partial U}{\partial X}+\frac{\partial V}{\partial Y}=0 \tag{1}$$

$$\frac{\partial U}{\partial \tau}+\frac{1}{Pr_0}\left(U\frac{\partial U}{\partial X}+V\frac{\partial U}{\partial Y}\right) = -\frac{\partial P}{\partial X}+\frac{\partial}{\partial X}\left[f(\Theta)\frac{\partial U}{\partial X}\right]+\frac{\partial}{\partial Y}\left[f(\Theta)\frac{\partial U}{\partial Y}\right] \tag{2}$$

$$\frac{\partial V}{\partial \tau}+\frac{1}{Pr_0}\left(U\frac{\partial V}{\partial X}+V\frac{\partial V}{\partial Y}\right) = -\frac{\partial P}{\partial Y}+\frac{\partial}{\partial X}\left[f(\Theta)\frac{\partial V}{\partial X}\right]+\frac{\partial}{\partial Y}\left[f(\Theta)\frac{\partial V}{\partial Y}\right] + Ra_0\Theta \tag{3}$$

$$\frac{\partial \Theta}{\partial \tau}+U\frac{\partial \Theta}{\partial X}+V\frac{\partial \Theta}{\partial Y}=\frac{\partial}{\partial X}\left[h(\Theta)\frac{\partial \Theta}{\partial X}\right] +\frac{\partial}{\partial Y}\left[h(\Theta)\frac{\partial \Theta}{\partial Y}\right] \tag{4}$$

The coefficients $f(\Theta)$ and $h(\Theta)$ represent in dimensionless form the temperature-dependent viscosity and thermal conductivity, respectively. For a fluid with constant properties $f(\Theta)=1.0$ and $h(\Theta)=1.0$, and for the glass melt $0.42\leqslant f(\Theta)\leqslant 14.72$ and $0.57\leqslant h(\Theta)\leqslant 1.23$ in the temperature range 1400–1800 K. The dimensionless variables that appear in equations (1)–(4), are

$$f(\Theta)=\frac{\mu(\Theta)}{\mu_0},\quad h(\Theta)=\frac{k(\Theta)}{k_0} \tag{5}$$

$$X=\frac{x}{H},\quad Y=\frac{y}{H},\quad U=\frac{uH}{\alpha_0},\quad V=\frac{vH}{\alpha_0} \tag{6}$$

$$\tau=\frac{tv_0}{H^2},\quad P=\frac{pH^2}{\rho\alpha_0 v_0},\quad \Theta=\frac{T-T_0}{\frac{q''H}{k_0}} \tag{7}$$

where, P and Θ are the non-dimensional pressure and temperature, respectively, and U and V are the

Table 1
Thermo-physical properties of a container glass-melt (after Muschick and Muysenberg [32] and Jian and Zhihao [17])

Symbol	Value (T in K)
ρ, kg/m^3	2300.0
c_P, J/(kg K)	1300.0
k_{eff}, W/(m K)	$5.386-2.168\times10^{-2}T+2.058\times10^{-5}T^2$
μ, kg/(m s)	$10.0^{\left(-2.58+\frac{4332}{T-521}\right)}$
β, K^{-1}	6.0×10^{-5}

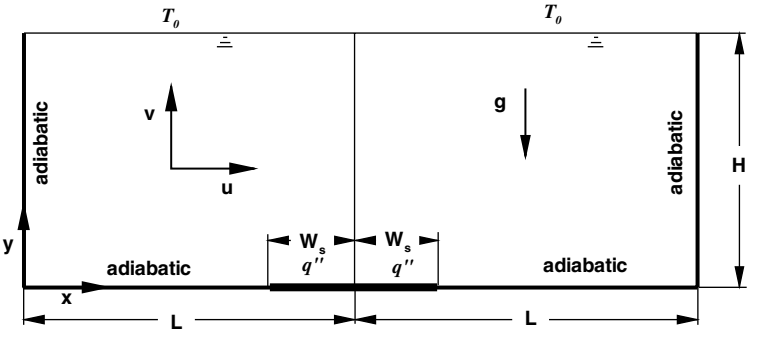

Fig. 1. Flow configuration and boundary conditions.

non-dimensional velocity components in the x- and y-directions, respectively. The subscript '0' indicates that the reference values for the properties are evaluated at the constant temperature of the free surface ($T_0 = 1400$ °C).

The characteristic parameters of the flow are the Rayleigh number ($Ra_0 = \frac{g\beta q'' H^4}{\nu_0 \alpha_0 k_0}$) based on the tank height H and the strip heat flux q'', and the Prandtl number ($Pr_0 = \frac{\nu_0}{\alpha_0}$). All Rayleigh numbers studied here may be encountered in industrial glass melting tanks, through control of the externally supplied electric current. The Prandtl number of the glass melt at the reference temperature was approximately 737.

The computations were performed using unsteady formulation on the half domain for the cases of low Rayleigh number and with the heated strip centred at the bottom wall. In all other cases, asymmetric heating at the bottom wall or high Raleigh numbers, the computations were carried out in the entire domain. The initial and boundary conditions for the entire solution domain and with the heated strip centred at the bottom wall are given below:

$$\tau = 0$$

$$U = V = \Theta = 0$$

$$\tau > 0$$

$$\frac{\partial U}{\partial Y} = V = \Theta = 0 \quad \text{at } Y = 1$$

$$U = V = \frac{\partial \Theta}{\partial X} = 0 \quad \text{at } X = 0$$

$$U = V = \frac{\partial \Theta}{\partial X} = 0 \quad \text{at } X = \frac{2L}{H} = 2A$$

$$U = V = \frac{\partial \Theta}{\partial Y} = 0 \quad \text{at } Y = 0 \text{ and } \begin{cases} 0 \leqslant X < \dfrac{(L - W_s)}{H} \\ \dfrac{(L + W_s)}{H} < X \leqslant \dfrac{2L}{H} \end{cases}$$

$$\left.\begin{array}{l} U = V = 0 \\ \dfrac{\partial \Theta}{\partial Y} = -1 \end{array}\right\} \quad \text{at } Y = 0 \text{ and } \frac{(L - W_s)}{H} \leqslant X \leqslant \frac{L + W_s}{H} \tag{8}$$

The zero reference value of the streamfunction Ψ (calculated from the velocity field using the relations $V = -\frac{\partial \Psi}{\partial X}$ or $U = \frac{\partial \Psi}{\partial Y}$) corresponds to the position $(X, Y) = (0, 0)$. The Nusselt number is calculated from the temperature field, using the values at the boundary and the next two interior grid nodes. The average Nusselt number at the heated strip is given by

$$\overline{Nu} = \frac{\overline{h} H}{k_0} = \frac{1}{\overline{\Theta}_s} \tag{9}$$

where, $\overline{\Theta}_s$ is the non-dimensional average temperature at the heated strip, calculated as

$$\overline{\Theta}_s = \frac{\overline{T}_s - T_0}{q'' H / k_0} \tag{10}$$

and, the average dimensional temperature at the heated strip, $\overline{T}_s$, is calculated as

$$\overline{T}_s = \frac{1}{W_s} \int_{L - W_s}^{L} T(x, 0)\, dx \tag{11}$$

The local heat transfer at the free surface of the tank is determined by the local Nusselt number:

$$Nu_{fs} = \frac{hH}{k} = -\frac{1}{\overline{\Theta}_s} \left.\frac{\partial \Theta}{\partial Y}\right|_{Y=1} \tag{12}$$

and the average Nusselt number at the free surface is given as

$$\overline{Nu}_{fs} = \frac{W_s}{L} \frac{1}{\overline{\Theta}_s} = \frac{W_s}{L} \overline{Nu} \tag{13}$$

indicating that the total heat supplied to the glass melt by the heated strip is equal to the total heat loss from the free surface.

3. Numerical procedure

The governing equations together with the corresponding boundary conditions are solved numerically, employing a finite-volume method. The SIMPLE method of Patankar and Spalding [18] is used to couple the momentum and continuity equations in a uniform staggered grid. In order to minimize numerical diffusion, the convective terms in the momentum and energy equations are discretized using the QUICK scheme of Leonard [19], in the modified form proposed by Hayase et al. [20]. The diffusion terms are discretized using central differences, while a second order accurate implicit scheme is used for the transient terms. In all calculations presented here, under-relaxation factors with values of 0.5, 0.5, 0.7 and 0.3 were applied to U, V, Θ and P, respectively.

Convergence within each time step is determined through the sum of the absolute relative errors for each dependent variable in the entire flow field:

$$\sum_{i,j} \frac{\left|\phi_{i,j}^{k+1} - \phi_{i,j}^{k}\right|}{\left|\phi_{i,j}^{k}\right|} \leqslant \varepsilon \tag{14}$$

where, ϕ represents the variables U, V or Θ, the superscript k refers to the iteration number and the subscripts i and j refer to the space coordinates. The value chosen for ε was 10^{-5}, for all calculations. Steady state is achieved when $\sum_{i,j} |\phi_{i,j}^{n+1} - \phi_{i,j}^{n}| \leqslant \varepsilon$, where n refers to the time iteration. Time steps from 10^{-5} to 10^{-6} were used to insure good accuracy in time and ability to capture instabilities if they exist. All calculations are carried out

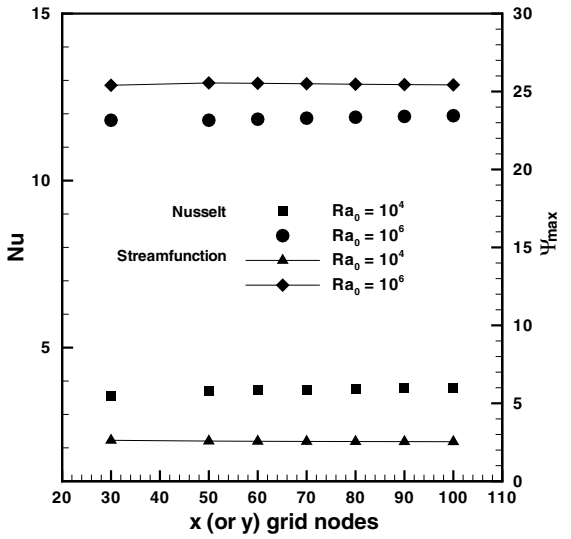

Fig. 2. Grid independence tests with respect to maximum Nu_{fs} at the free surface and maximum streamfunction value.

on Intel CPU based personal computers using the in-house CFD code GLASS3D, [21].

The present numerical model was validated against the benchmark numerical solution of De Vahl Davis [22] for natural convection of air in a square cavity. These results in the case of $Ra = 10^6$ showed relative differences of 0.1% and 0.06% for the streamfunction values at the centre of the cavity and the average Nusselt number, respectively. It was also validated against the numerical results of Canzarolli and Milanez [23] for the case of natural convection in a shallow enclosure ($L/H = 7$) heated from below at constant heat flux and cooled from the sidewalls. The relative differences observed in the maximum value of streamfunction and the average Nusselt number, at the highest Rayleigh number of 10^6 studied, were 0.5% and 0.04%, respectively. Finally, the model was tested against the work of Emery and Lee [9] for natural convection in a square enclosure with both temperature-dependent viscosity and thermal conductivity, for the case of $Ra_0 = 10^5$. At the dimensionless height of $Y = 0.743$, the maximum relative difference was found to be 0.01% for the temperature and less than 0.4% for the vertical velocity component.

Prior to the final computations, grid independence tests were performed for every tank aspect ratio, A, studied. For the square half-tank, the representative case of $A_s = 0.2$ was tested for $Ra_0 = 10^4$ and 10^6, using uniform grid sizes of 30×30 to 100×100, in both x- and y-directions of the half tank. As shown in Fig. 2, the variation of the maximum local Nusselt number at the free surface appears to be negligible, and for grid sizes larger than 80×80 the variation of the maximum stream function are less than 0.1%. For these reasons, the 80×80 uniform grid was selected for all calculations in the present study. For the shallow tank, a uniform grid of 80 nodes was adopted in the y-direction for both tank aspect ratios ($A = 3$ and 7) with 140 nodes for $A = 3$ and 200 nodes for $A = 7$ in the x-direction. These selected grids resulted in differences less than 0.8% for the maximum local Nusselt number at the free surface and maximum value of streamfunction from finer grids.

In order to determine possible three-dimensional effects, computations were performed for a three-dimensional tank with width equal to the height. In the

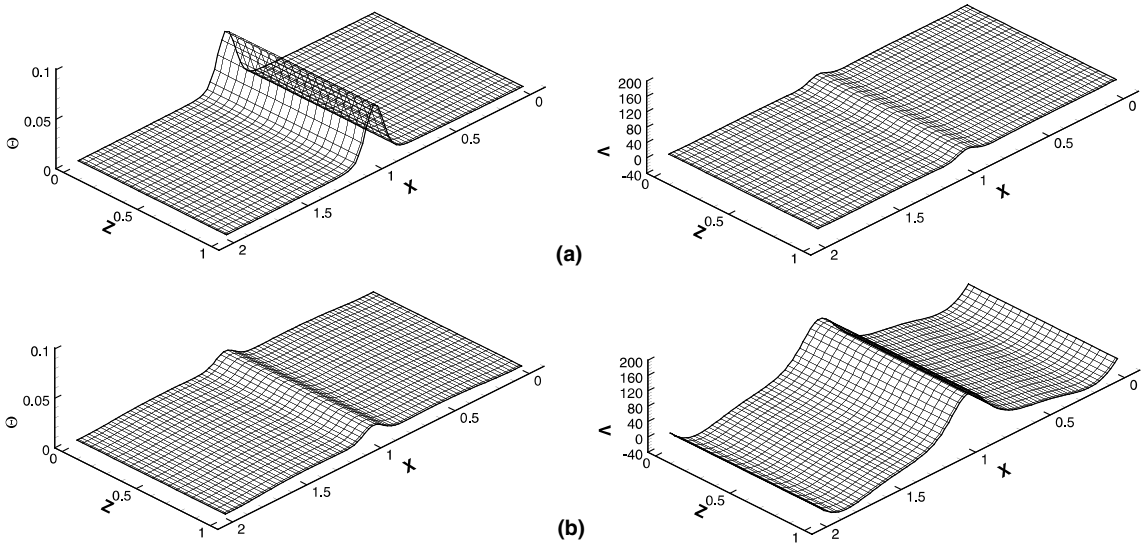

Fig. 3. Temperature and vertical velocity distributions for $Ra_0 = 10^6$, $A = 1$ and $A_s = 0.1$ along horizontal planes: (a) $Y = 0.045$, and (b) $Y = 0.365$.

z-direction, symmetry conditions were considered and the grid employed was uniform of size $160\times80\times40$. Indicative results for the case of $Ra_0 = 10^6$, $A = 1$ and $A_s = 0.1$ are presented in Fig. 3, where temperature and vertical velocity distributions along planes parallel to the bottom wall are shown. These results show clearly that the heated strip does not produce significant three-dimensional effects in the range of parameters studied. This behaviour applies to all flow properties and is in agreement with the stability analysis of the glass-melting tank by Lim et al. [24]. Comparison of their results based on two-dimensional steady-state computations with those from two- and three-dimensional unsteady computations shows no observable differences. For these reasons, two-dimensional computations were performed in the present study. Numerical experiments also conducted in a tank with rigid sides showed no three-dimensional effects for the Rayleigh numbers used in the present simulation.

4. Results

The present numerical results were obtained for a range of Rayleigh numbers from 10^2 to 10^7, tank aspect ratios $A = 1.0$, 3.0 and 7.0 and strip width to tank length ratios $A_s = 0.1$, 0.2, 0.3, 0.4 and 0.5. The flow and temperature fields in the tank are shown in the form of streamlines and isotherms, with 15 equally spaced contour levels. The streamline levels are between the respective maximum value and zero and the temperature levels range between the zero value at the free surface and the highest value corresponding to the heated strip region.

4.1. Square half-tank with symmetric heating

Figs. 4–9 show the results corresponding to the square half-tank ($A = 1$) where the heated strip is centred on the bottom wall of the tank. The flow just above the strip ascends towards the cold free surface, then moves horizontally towards the corner of the tank, descends to the bottom of the tank and finally returns to the heated strip region. Fig. 4 shows the streamlines and isotherms for different Rayleigh numbers and a heated strip width to tank length ratio $A_s = 0.1$. When $Ra_0 = 10^2$, the isotherms are almost concentric circles around the heated strip, because heat is transferred to the fluid body by pure conduction. As the Rayleigh number increases, and consequently the fluid starts to circulate, the convective mode of heat transfer starts to dominate over that of conduction. This increase in the circulation intensity results in a decrease of the fluid temperature. The free surface, the sidewall and the part of the bottom wall not covered by the heated strip have almost the same low temperature ($\Theta = 0$) whereas the temperature gradients are concentrated just above the heated strip, where a thermal plume is formed. In the highest Rayleigh number cases studied (i.e. $Ra_0 = 10^6$, 10^7) the isotherms show significant curvature just above the heated strip.

Fig. 5 shows the dimensionless temperature distribution, for strip width ratio $A_s = 0.1$ along the bottom wall (a) and the symmetry plane (b). The almost similar temperature distributions corresponding to the lower Rayleigh numbers of 10^2 and 10^3 indicate that heat transfer is mainly due to conduction. The maximum temperature of approximately 0.24 occurs at the centre of the heated strip and corresponds to the pure conduction limit. With increasing Rayleigh number, the temperature at the bottom wall not covered by the heated strip, decreases and, at $Ra_0 = 10^7$, it becomes almost zero. From the temperature distribution along the symmetry plane for all cases studied, a conduction thermal boundary layer is shown to exist adjacent to the free surface. This layer covers approximately 30% of the fluid depth for $Ra_0 = 10^4$, 10% for $Ra_0 = 10^5$ and less than 5% for $Ra_0 = 10^6$ and 10^7. Chu and Hickox [6] observed also this surface conduction layer to have a thickness of approximately 15% for Rayleigh numbers of the order of 10^4.

The distribution of local Nusselt number at the free surface, for the case $A_s = 0.1$ and for all the Rayleigh numbers studied, is shown in Fig. 6. The positive sign indicates that heat is lost from the fluid. For the lower Raleigh numbers, no significant variations across the surface are observed due to the pure conduction heat transfer. For higher Rayleigh numbers, the free surface heat transfer rate is maximum near the symmetry plane due to the rising plume and minimum at the sidewalls. Increasing the Rayleigh number increases the maximum values of the local Nusselt number at the free surface above the heated strip.

The effect of heated strip width to tank length ratio A_s on the flow and heat transfer is illustrated in Fig. 7, for the convection-dominated case of $Ra_0 = 10^6$ and the range of $A_s = 0.2$–0.5 (the case $A_s = 0.1$ was shown in Fig. 4). Increasing A_s, does not result in significant changes of the flow patterns but intensifies the circulation zones and increases the maximum fluid temperature. The strip width affects strongly the temperature distribution within the body of the fluid, but causes insignificant changes near the sidewall.

The influence of the Rayleigh number on the present natural convection flow can be explained qualitatively on pure scaling arguments (see [23,25,26]). In the following analysis, all quantities are estimated at the reference temperature. As shown in Fig. 4, at high enough Rayleigh numbers the flow along and above the heated strip forms two boundary layers. A thermal boundary layer is formed along the heated strip which turns into a buoyant thermal plume centred on top of the strip. The

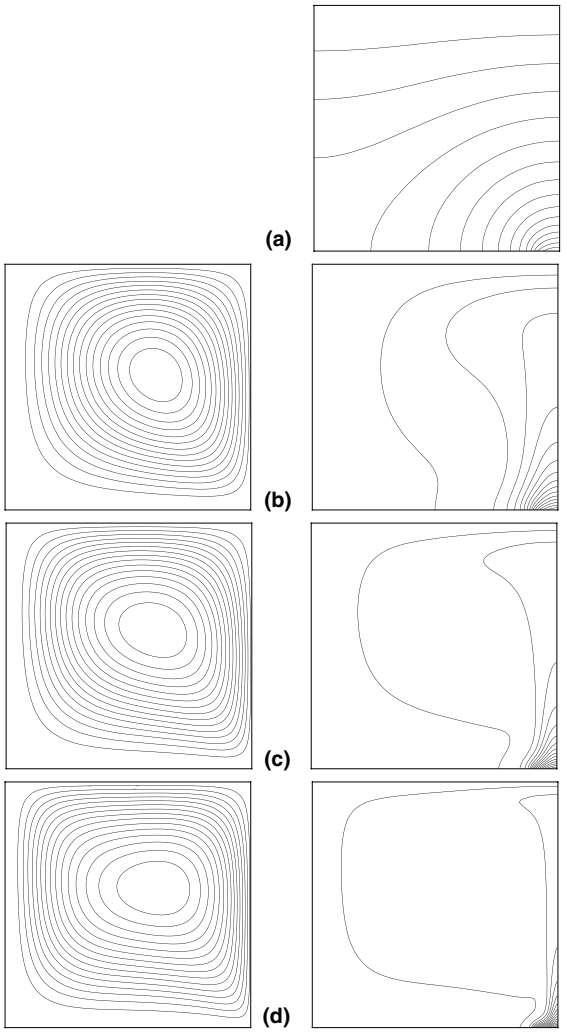

Fig. 4. Streamlines and isotherms for $A = 1$, $A_s = 0.1$: (a) $Ra_0 = 10^2$ ($\Psi_{max} = 0.0$, $\Theta_{max} = 0.24$); (b) $Ra_0 = 10^5$ (6.48, 0.14); (c) $Ra_0 = 10^6$ (18.77, 0.094); (d) $Ra_0 = 10^7$ (52.208, 0.06).

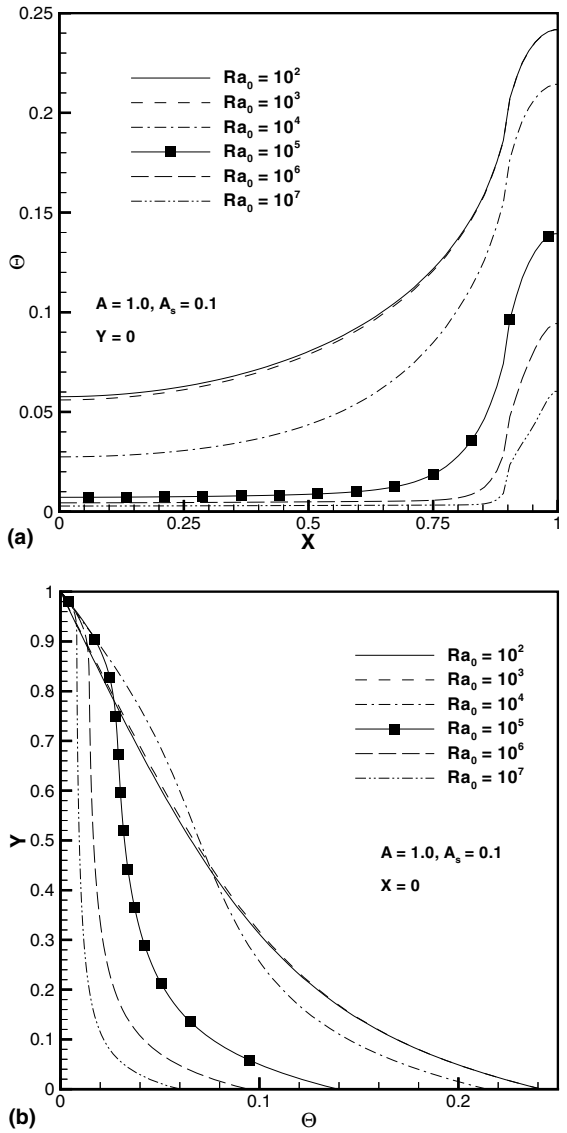

Fig. 5. Temperature distribution in the square half-tank for different values of Ra_0 and $A_s = 0.1$ along: (a) the bottom wall, and (b) the symmetry plane.

initiation of this flow can be understood by considering the simpler problem of a heated horizontal plate in a fluid of infinite extent. This problem, for the case of constant uniform temperature, has been studied extensively by, for example, Goldstein and Lau [27], Rotem and Claassen [28] and Lewandowski [29], and relatively less for constant heat flux by Pera and Gebhart [30] and Chen et al. [31]. In this kind of heating, the flow is drawn inwards from the two edges of the heated strip forming boundary layers along its surface which may meet at the centre of the strip before they turn through a right angle and form a thermal plume. If the strip width were sufficiently wide and its heating rate very high, the local buoyancy will cause the boundary layers to separate prior to the strip centre. The latter is unlikely to occur in the present flow configuration. The flow inwards is caused entirely by the lower pressure levels towards the strip centre which are induced entirely by the buoyancy force away from the surface.

Using the boundary layer momentum and energy equations for a Prandtl number value of 1 or greater and pure scaling arguments (according to which the pressure gradient term balances the buoyant term in the y-momentum equation, the pressure gradient term balances the viscous term in the x-momentum equation, and the inertial term balances the diffusion term in the energy equation) leads to a Nusselt–Rayleigh number dependence: $(Ra_{W_s})^{1/5}$ for an isothermal plate, and

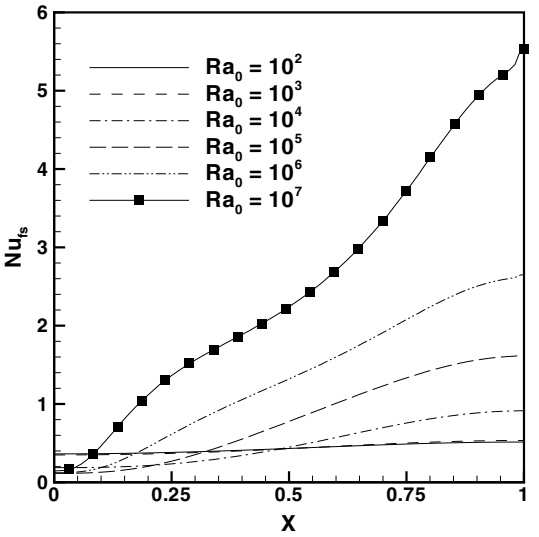

Fig. 6. Distribution of Nu_{fs} along the free surface for $A = 1$, $A_{\mathrm{s}} = 0.1$, and different values of Ra.

$(Ra_{W_{\mathrm{s}}})^{1/6}$ for a constant heat flux plate (present study). The results of this remarkably simple analysis, agree in form with the analytic results of Chen et al. [31]. The above modified Rayleigh number is based on the strip width W_{s} as characteristic length.

Because, in the present problem the fluid is of finite extent, the rising fluid in the thermal plume will have to return to the bottom to replace that already risen, resulting in a recirculation pattern. The sense of the recirculation is such that the flow along the bottom wall is in the same direction as that induced by the buoyancy forces corresponding to the infinite fluid, when the fluid starts moving from rest. This fluid motion is expected to result in a thinner thermal boundary, which in turn is expected to increase the rate of heat transfer.

Using pure scaling arguments again as in [25] for both the thermal boundary layer and the plume and with $Pr = 1$ or greater leads to the following scaling laws:

(a) For the energy equation in the thermal boundary layer of thickness δ_{t} over the strip having a temperature difference ΔT:

$$\text{Longitudinal convection } \frac{u\Delta T}{W_{\mathrm{s}}} \sim \text{Transverse diffusion } \alpha\frac{\Delta T}{\delta_{\mathrm{t}}^2} \tag{15}$$

(b) For the u-momentum equation within the thermal boundary layer over the strip:

$$\text{Pressure gradient } \frac{\Delta P}{W_{\mathrm{s}}} \sim \text{Viscous forces } \frac{\mu u}{\delta_{\mathrm{t}}^2} \tag{16}$$

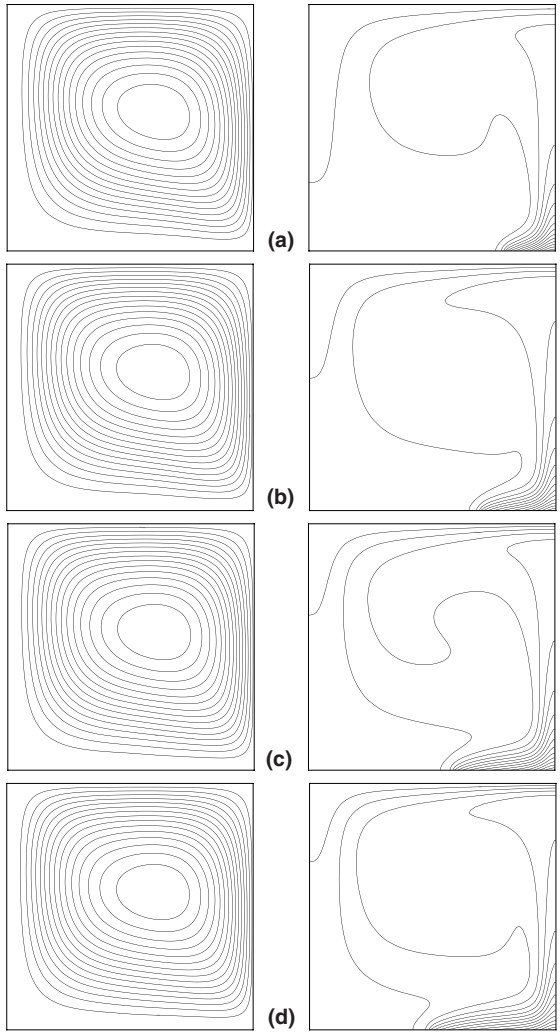

Fig. 7. Streamlines and isotherms for $Ra_0 = 10^6$, $A = 1$: (a) $A_{\mathrm{s}} = 0.2$ ($\Psi_{\max} = 25.468$, $\Theta_{\max} = 0.117$), (b) $A_{\mathrm{s}} = 0.3$ (30.59, 0.132), (c) $A_{\mathrm{s}} = 0.4$ (34.98, 0.144), (d) $A_{\mathrm{s}} = 0.5$ (38.86, 0.154).

In the lower region of the plume, where the temperature is high, the viscosity of the glass-melt could be approximately 35 times smaller than that away from the heated strip and thus, the viscous forces are not expected to be very important. In this region, the plume is subjected to strong acceleration as was observed experimentally by Katsavos et al. [8] using a glycerol solution (a fluid with similar viscosity behaviour to the glass-melt). Based on this discussion, it is expected, that in the lower region of the plume, the pressure gradient in the vertical direction is of the same order with the buoyancy forces and the inertial forces, i.e.:

$$\frac{\Delta P}{H} \sim \rho\frac{v^2}{H} \sim \rho g\beta\Delta T \tag{17}$$

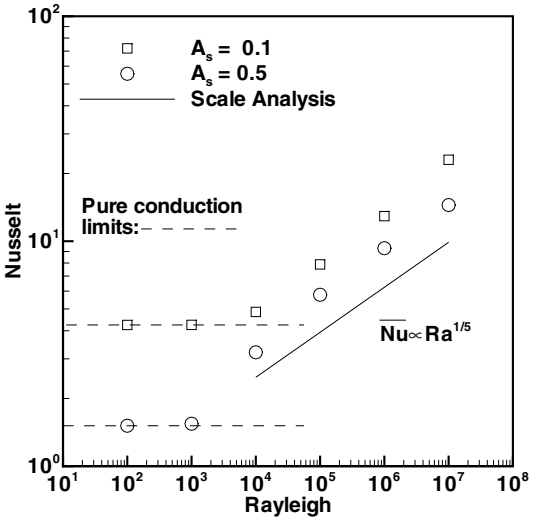

Fig. 8. Variation of $\overline{Nu}$ at the heated strip as a function of Ra_0 for $A = 1$ ($A_s = 0.1$ and 0.5).

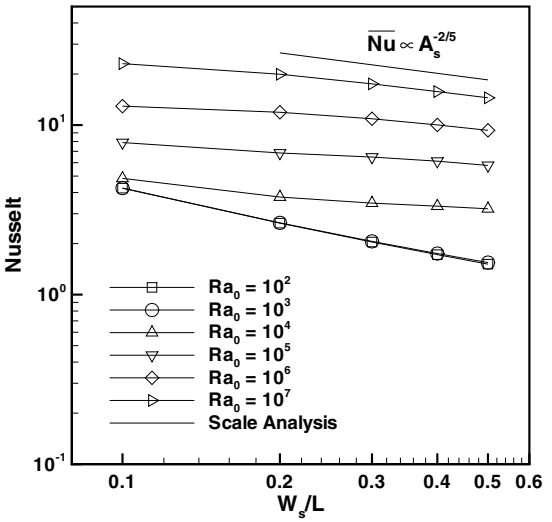

Fig. 9. Variation of $\overline{Nu}$ at the heated strip for $A = 1$ as a function of A_s at different R_0.

The pressure rise at the centre of the heated strip on the wall region where the plume stagnates is

$$\Delta P \sim \rho v^2 \tag{18}$$

and from mass continuity

$$v\delta_p \sim u\delta_t \tag{19}$$

where δ_p is the width of the plume.

Eqs. (15)–(19) are sufficient for determining the unknown scales. Of particular interest are the resulting scaling laws for the thickness δ_t, and the velocity u in the thermal boundary layer along the width of the strip:

$$\delta_t \sim H\left(\frac{W_s}{H}\right)^{1/2} Ra_T^{-1/4} \tag{20}$$

$$u \sim \frac{\alpha}{H} Ra_T^{1/2} \tag{21}$$

for a strip at uniform temperature with the Rayleigh number defined as $Ra_T = \frac{g\beta\Delta T H^3}{\nu_0 \alpha_0}$, where ΔT the difference between the temperature of the strip and T_0, and

$$\delta_t \sim H\left(\frac{W_s}{H}\right)^{2/5} Ra_0^{-1/5} \tag{22}$$

$$u \sim \frac{\alpha}{H}\left(\frac{W_s}{H}\right)^{1/5} Ra_0^{2/5} \tag{23}$$

for a heated strip of uniform flux, as in the present study.

The maximum value of the streamfunction ψ_{max} is of the order of $u\delta$, where δ is the velocity boundary layer thickness along the heated strip. For the case of $Pr \gg 1$, the velocity boundary layer thickness δ is of the order: $\delta \approx \delta_t Pr^{1/2}$.

Thus, we have

For constant temperature:

$$\psi_{max} \sim \alpha\left(\frac{W_s}{H}\right)^{1/2} Ra_T^{1/4} Pr^{1/2} \tag{24}$$

and for constant flux:

$$\psi_{max} \sim \alpha\left(\frac{W_s}{H}\right)^{3/5} Ra_0^{1/5} Pr^{1/2} \tag{25}$$

Finally, from the total heat rate ($Q \approx q'' W_s$) entering the tank bottom from the heated strip, the average Nusselt number over the heated strip can be expressed as

Constant temperature:

$$\overline{Nu} \sim \left(\frac{W_s}{H}\right)^{-1/2} Ra_T^{1/4} = (A_s A)^{-1/2} Ra_T^{1/4} \tag{26}$$

Constant flux:

$$\overline{Nu} \sim \left(\frac{W_s}{H}\right)^{-2/5} Ra_0^{1/5} = (A_s A)^{-2/5} Ra_0^{1/5} \tag{27}$$

Owing to the fact that $\delta_t \ll W_s$, the domain in which the scale analysis is valid can be determined from Eqs. (20) and (22):

Constant temperature:

$$\left(\frac{W_s}{H}\right)^{1/2} Ra_T^{1/4} = (A_s A)^{1/2} Ra_T^{1/4} \gg 1 \tag{28}$$

Constant flux:

$$\left(\frac{W_s}{H}\right)^{2/5} Ra_0^{1/5} = (A_s A)^{2/5} Ra_0^{1/5} \gg 1 \quad (29)$$

These relations represent the necessary criteria for the existence of a thermal boundary layer along the heated strip and a thermal buoyant plume above it.

The verification of the validity of the above scaling arguments is demonstrated with the numerical results of Fig. 8, where the Nusselt number is plotted as a function of Ra_0 for the strip width ratios of 0.1 and 0.5. The relation $\overline{Nu} \propto Ra^{1/5}$ is satisfied in almost all the range of the Rayleigh number that satisfies the criterion $(A_s A)^{2/5} Ra^{1/5} \gg 1$. For $A_s = 0.1$ and 0.5, the relation (27) is valid for $Ra \gg 10^2$ and 4, respectively, which results from satisfying the inequality (29). This is very well illustrated in Fig. 8 where for $Ra_0 = 10^3$, only the case $A_s = 0.5$ follows the relation (27). For lower Rayleigh numbers the criterion (29) is not satisfied, and the Nusselt number remains practically constant, as the heat transfer is dominated mainly by conduction. The horizontal dashed lines show the corresponding Nusselt numbers for the pure conduction.

The influence of both Rayleigh number and heated strip width A_s on the Nusselt number is shown in Fig. 9. As expected, the increase of Ra_0 increases the heat transfer in all cases, while the increase of A_s results in a decrease of Nusselt number. The last observation is connected with the fact that as the supplied heat from the heated strip for a given Ra_0 remains the same, the wider the heated strip the lower the heat transfer rate is. This variation is almost identical for the two lower Rayleigh numbers studied because of domination of conduction, and it is quite different from the higher Ra_0 cases, where convection becomes significant. For the pure conduction case, when the heated strip covers the entire bottom of the tank ($A_s = 1$), the Nusselt number has the value of 1.

4.2. Shallow tank with symmetric heating

Fig. 10 shows the streamlines and isotherms at different Rayleigh numbers for a tank with $A = 3$ and a heated strip width $A_s = 0.1$. As in the previous case, the flow consists of a single cell that rotates counterclockwise. However, in this case, the cell does not occupy the whole extent of the tank, especially for intermediate Ra_0. For very small values of Ra_0 the heat transfer is only due to pure conduction. As the Rayleigh number increases and thus convection increases, the circulation cell

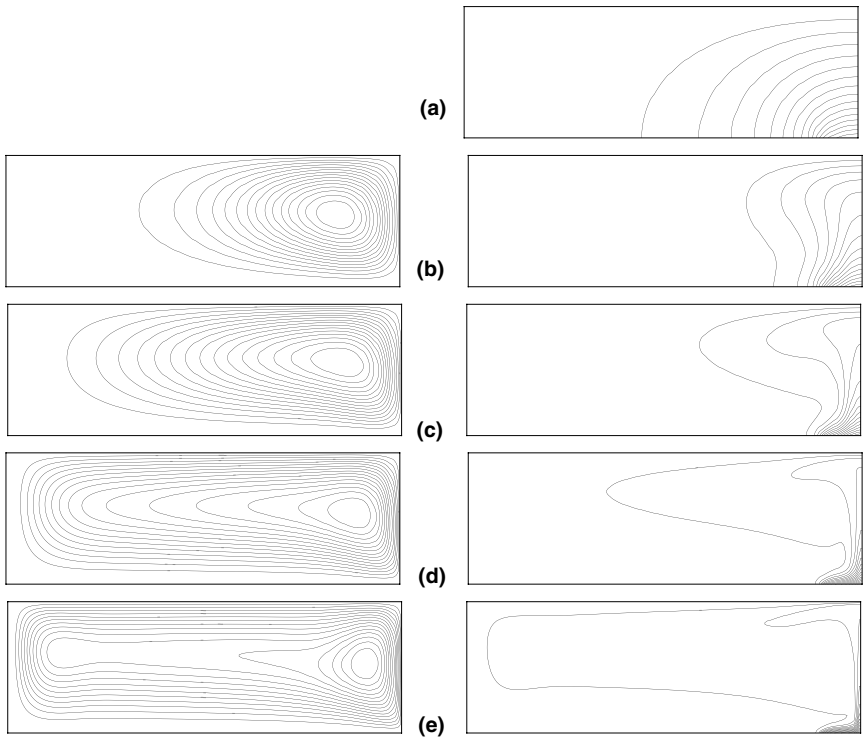

Fig. 10. Streamlines and isotherms for $A = 3$, $A_s = 0.1$: (a) $Ra_0 = 10^2$ ($\Psi_{max} = 0.0$, $\Theta_{max} = 0.47$), (b) $Ra_0 = 10^4$ (3.756, 0.313), (c) $Ra_0 = 10^5$ (11.134, 0.194), (d) $Ra_0 = 10^6$ (28.087, 0.122), (e) $Ra_0 = 10^7$ (77.328, 0.075).

shrinks and this process continues until the Ra_0 reaches the value of 10^4. Further increase in the Rayleigh number causes convection to dominate over conduction and as a result the circulation cell expands to occupy the entire tank.

The temperature fields show the existence of two well defined regions, a cold uniform temperature region and a hot region. A thermal penetration length can be defined which represents the horizontal distance from the vertical plane passing through the centre of the heated strip which is affected by the thermal plume. For comparison purposes, this distance is determined by the furthest point of the lowest value isotherm (level value is 1/15). A thermal penetration due to convection appears at approximately $Ra_0 = 10^4$, while at $Ra_0 = 10^5$, the thermal penetration occupies more than one-third of the tank length; at $Ra_0 = 10^6$, occupies approximately two-thirds of the tank length; and at $Ra_0 = 10^7$, reaches almost the sidewall of the tank. This thermal penetration length concept has also been studied, among others, by Poulikakos [26] and Ganzarolli and Milanez [23], but was based on an isotherm value of 1/10. Increase of the Rayleigh number makes the thermal plume stronger and slender, as in the square half-tank case.

The influence of the heated strip width ratio A_s on the flow and heat transfer characteristics for $A = 3$ and $Ra_0 = 10^6$ is illustrated in Fig. 11 (the value of $A_s = 0.1$ was already illustrated in Fig. 10). The circulation patterns are not affected significantly by A_s, but the maximum streamfunction value, which is a measure of their intensity, is increased by a factor of 2 between $A_s = 0.1$ and 0.5. The temperature distribution inside the fluid body is strongly affected by A_s, especially near the heated strip, as in the corresponding square half-tank case.

The effect of Rayleigh number and heated strip width ratio A_s on the Nusselt number for a tank with $A = 3$ is shown in Fig. 12. Increasing A_s, the Nusselt number decreases as in the square half-tank case. The Nusselt number corresponding to a given A_s increases also with increasing Rayleigh number. For the two smaller Ra_0 studied, heat transfer is dominated mainly by

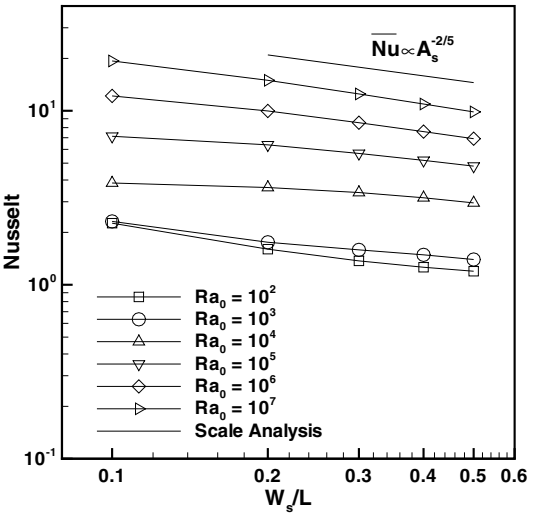

Fig. 12. Variation of $\overline{Nu}$ at the heated strip for $A = 3$, as a function of A_s at different Ra_0.

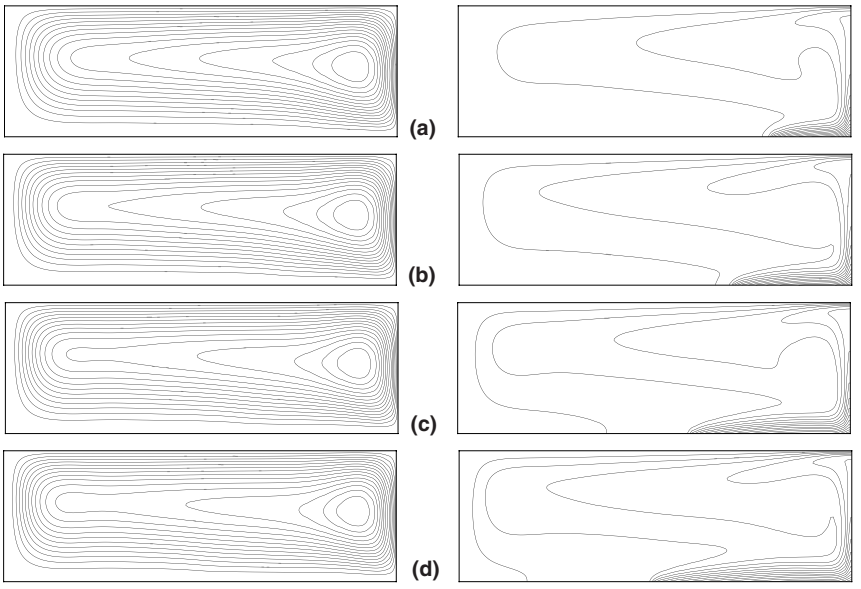

Fig. 11. Streamlines and isotherms for $Ra_0 = 10^6$, $A = 3$: (a) $A_s = 0.2$ ($\Psi_{max} = 38.335$, $\Theta_{max} = 0.148$), (b) $A_s = 0.3$ (45.756, 0.167), (c) $A_s = 0.4$ (51.609, 0.183), (d) $A_s = 0.5$ (56.585, 0.197).

conduction and the $\overline{Nu}$ vs. A_s curves are relatively close to each other, especially for small A_s. However, for $Ra_0 = 10^3$, as A_s increases, a weak contribution from convection causes the small differences observed.

The flow and temperature fields for the most shallow tank studied ($A = 7$) with $A_s = 0.1$ and different Ra_0 values are shown in Fig. 13. The region where the temperature is affected by the strip is large at low Ra_0 due to conduction and shrinks initially with the Ra_0 until a thermal plume is formed at approximately $Ra_0 = 10^4$. This plume becomes more slender by further increasing the Rayleigh number and simultaneously the temperature penetration length is increased as a result of the influence of the free surface. At the highest Rayleigh number the thermal penetration approaches the tank sidewall. As previously observed (case $A = 3$) the extent of the circulation cell increases monotonically with increasing Ra_0 in the pure convective regime of $Ra_0 > 10^4$.

The flow and temperature fields for strip width values $A_s = 0.2$ to 0.5 and for $Ra_0 = 10^6$ are shown in Fig. 14. The circulation cell seems to be of larger extent and more intense with increasing A_s, as previously observed for the other tank aspect ratios. The thermal penetration length increases also with increasing A_s and, for the largest value it reaches almost the sidewall. In principle, both parameters Ra_0 and A_s can increase the heat transfer in a tank of specified aspect ratio A, in accordance with Eq. (27). However, an important aspect of glass production process, which affects the quality of the final product, is homogenization of the glass melt. This becomes possible through the existence of circulation currents in the tank and uniform temperature fields, avoiding the formation of cold regions. Comparing the flow and temperature fields in Figs. 10 and 13, which correspond to fixed A_s with variable Ra_0, with the respective Figs. 11 and 14 which correspond to fixed Ra_0 with variable A_s, we observe by increasing A_s that: (a) the

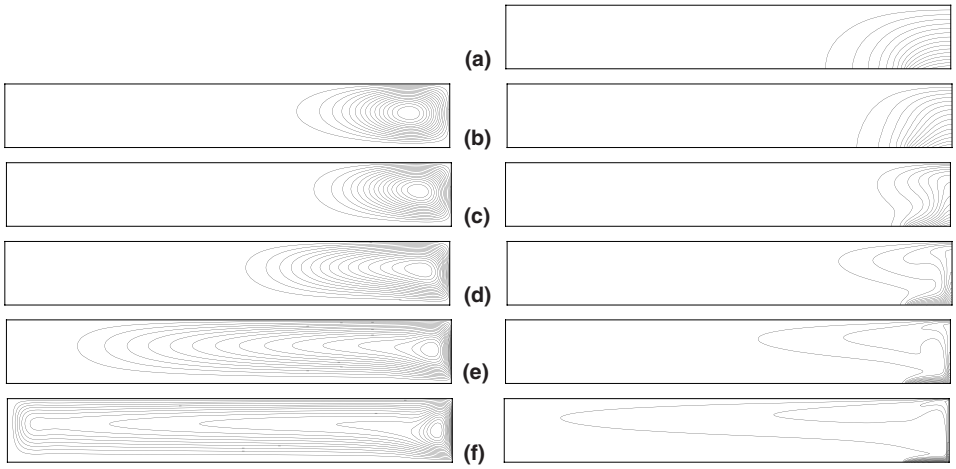

Fig. 13. Streamlines and isotherms for $A = 7$, $A_s = 0.1$: (a) $Ra_0 = 10^2$ ($\Psi_{max} = 0.0$, $\Theta_{max} = 0.734$), (b) $Ra_0 = 10^3$ (1.131, 0.715), (c) $Ra_0 = 10^4$ (5.875, 0.406), (d) $Ra_0 = 10^5$ (15.933, 0.244), (e) $Ra_0 = 10^6$ (40.247, 0.149), (f) $Ra_0 = 10^7$ (111.475, 0.089).

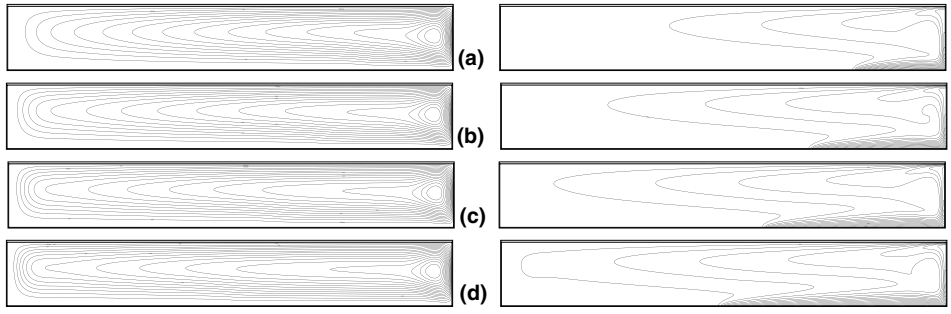

Fig. 14. Streamlines and isotherms for $Ra_0 = 10^6$, $A = 7$: (a) $A_s = 0.2$ ($\Psi_{max} = 53.546$, $\Theta_{max} = 0.183$), (b) $A_s = 0.3$ (62.898, 0.208), (c) $A_s = 0.4$ (70.309, 0.229), (d) $A_s = 0.5$ (76.503, 0.248).

circulation current is stronger as indicated by the peak streamline values and of larger extent covering the entire half of the tank, which in turn promotes mixing and homogenization of the glass melt, and (b) the isotherms show that the increase of A_s raises the temperature in the entire tank, thus avoiding the presence of cold regions and the possibility of local solidification of the melt. This temperature field contributes further to the homogenization of the glass melt. The increase in Rayleigh number (through increasing the heat flux rate q'' and consequently the operational costs) increases mainly the temperature locally above the heated strip. Based on the above arguments, it seems that the most effective way of increasing flow circulation currents and temperature of the glass melt is by increasing A_s for all tank aspect ratios studied.

The dependence of the Nusselt number on the Rayleigh number for different tank aspect ratios and the fixed value of $A_s = 0.1$ is shown in Fig. 15. The $\overline{Nu} \propto Ra^{1/5}$ relation describes well the heat transfer by convection, for all the tank aspect ratios and for all Rayleigh numbers studied. For low Rayleigh numbers the heat transfer is due to conduction and, thus, the Nusselt numbers remain unchanged. The Nusselt numbers corresponding to pure conduction are shown in Fig. 15 by the horizontal dashed lines. For this range of Rayleigh numbers the criterion of validity of the scale analysis, Eq. (29), is not satisfied anymore. For $A = 1$, 3 and 7, this criterion gives that Eq. (27) is approximately valid for $Ra_0 \gg 10^2$, 11 and 2, respectively.

Finally, the effect of tank aspect ratio on the Nusselt number for different Rayleigh numbers and a fixed value $A_s = 0.1$ is shown in Fig. 16. The $\overline{Nu}$ decreases almost linearly on a log–log plot with the tank aspect ratio and with approximately the same slope for $Ra_0 \geqslant 10^4$ (convective regime) as is indicated by Eq. (27). As shown in Fig. 16, for $Ra_0 = 10^2$ and all aspect ratios studied, the Nusselt number approximates the conductive regime, whereas for $Ra_0 = 10^3$ at some aspect ratios heat transfer is due to pure conduction and at some others to a mixed mode. For $Ra_0 = 10^3$, a mixed mode behaviour when increasing the tank aspect ratio occurs for $A > 2$. This demonstrates the influence of A on the initiation of convective currents, as implied by Eq. (27). The slope of the curve Nusselt number vs. A curve is different than $-\frac{2}{5}$ as expected, because heat transfer is not yet due mainly to the convection.

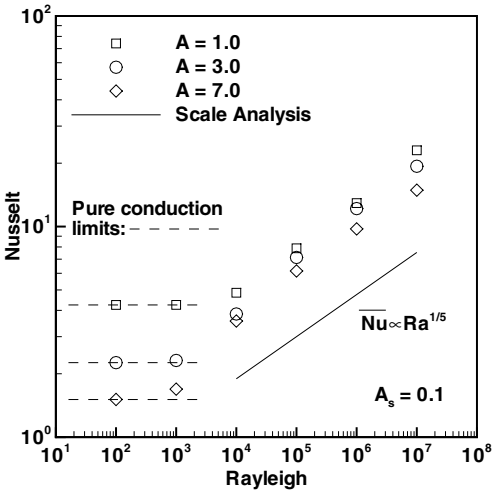

Fig. 15. Variation of $\overline{Nu}$ at the heated strip with $A_s = 0.1$ as a function of Ra_0 at different aspect ratios A.

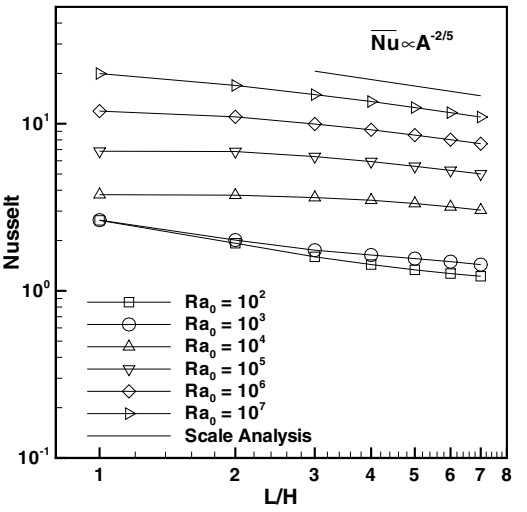

Fig. 16. Variation of $\overline{Nu}$ at the heated strip with $A_s = 0.1$ as a function of A at different Ra.

4.3. Non-symmetric heating

The heated strip is placed successively at the tank centre (i.e. $\frac{1}{2}L_t$) and to the right of the centre in increments of $\frac{1}{12}L_t$. The cases studied include all Ra_0, ant the A and A_s ranges as in the symmetric heating cases. The recirculation patterns and temperature fields for the representative case of $Ra_0 = 10^6$, $A = 3$ and $A_s = 0.1$ are shown in Fig. 17 with the heating strip centred at positions $\frac{1}{2}L_t$, $\frac{8}{12}L_t$ and $\frac{11}{12}L_t$. When the strip position is close to the tank centre, the familiar double cell flow pattern does appear. The extent of each of the two cells, as well as the resulting temperature penetration length are completely controlled by the strip position. As the strip approaches the adiabatic sidewall, the smaller circulation cell disappears while the other cell covers the entire tank, resulting in a small increase of the maximum fluid temperature.

The effect of the heated strip position on the heat transfer at the free surface of the tank (expressed in the form of local Nusselt number distribution) is shown in Fig. 18. The peak value of the local Nu_{fs} is considerably

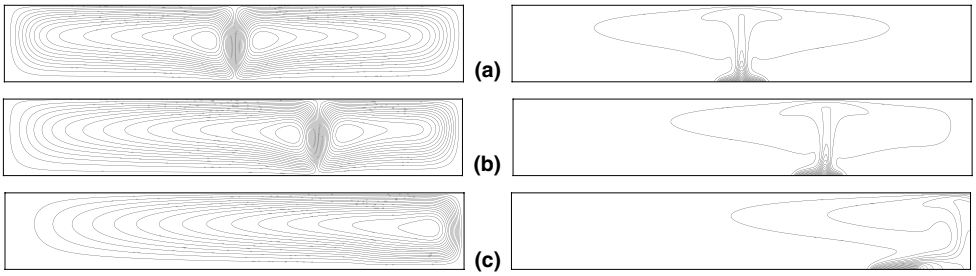

Fig. 17. Streamlines and isotherms for $Ra_0 = 10^6$, $A = 3$, $A_s = 0.1$ with strip placed at position: (a) $\frac{1}{2}L_t$ ($\Psi_{max} = 28.087$, $\Psi_{min} = -28.087$, $\Theta_{max} = 0.122$), (b) $\frac{8}{12}L_t$ (26.798, 29.541, 0.124), (c) $\frac{10}{12}L_t$ (34.266, 0.0, 0.130).

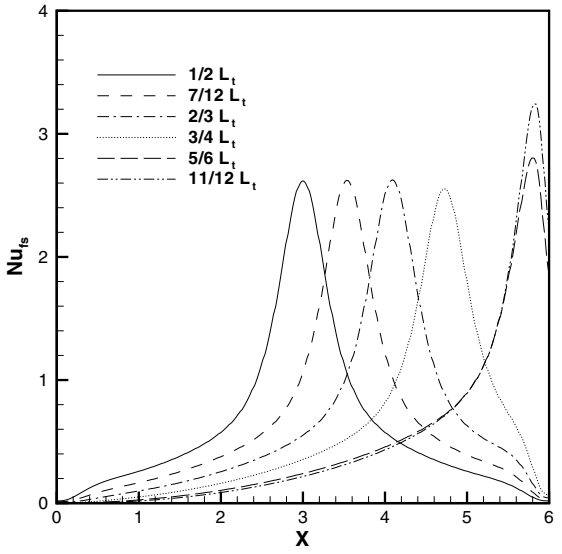

Fig. 18. Distribution of Nu_{fs} along the free surface for $Ra_0 = 10^6$, $A = 3$, $A_s = 0.1$, and for different heated strip positions.

higher, when the heated strip is placed closer to the sidewall.

5. Conclusions

A numerical study was presented of the buoyancy-induced flow and heat transfer in a two-dimensional open tank with localized heating from below and cooling from the free surface using a high Pr fluid. The influencing parameters are the Rayleigh number, the tank aspect ratio and the heated strip width. From the results presented and discussed above, the following may be concluded:

- For small Rayleigh numbers, the heat transfer is dominated by conduction, while at higher Ra_0 convection becomes dominant.
- For shallow tanks with symmetric heating, increasing the Rayleigh number results in an increase of the thermal penetration length from the symmetry plane to the sidewall. However, the increase of Ra_0 causes local increase of the temperature above the heated strip without noticeable increase of the temperature in the colder regions of the tank.
- Increase of the tank aspect ratio and the heated strip width intensifies the fluid flow and increases the temperature of the fluid. This makes the glass-melt more homogeneous resulting in better quality of the final product.
- A scale analysis, which gives $\overline{Nu} \sim (A_s A)^{-2/5} Ra_0^{\frac{1}{5}}$, agrees very well with the numerical results. This scale analysis was carried also for a constant temperature heated strip resulting to a $\overline{Nu} \sim (A_s A)^{-1/2} Ra_T^{1/4}$ relationship.
- The position of the heated strip plays also a role on the flow currents, the temperature distribution in the glass melt and the thermal penetration. Placing the heated strip near the adiabatic side wall results in a single cell with a consequent reduction in thermal penetration.

Acknowledgements

This work was partially funded by the General Secretariat for Research and Technology of Greece (research contract EPET-II/296). The leading author is grateful to the Research Board of the University of Thessaly for a research grant (EE 2418). The authors are grateful to the reviewers of this manuscript for their constructive criticism that have influence its quality.

References

[1] K.E. Torrance, J.A. Rockett, Numerical study of natural convection in an enclosure with localized heating from below—creeping glow to the onset of laminar instability, J. Fluid Mech. 36 (1969) 33–54.

[2] K.E. Torrance, L. Orloft, J.A. Rockett, Experiments on natural convection in enclosures with localized heating from below, J. Fluid Mech. 36 (1969) 21–31.
[3] S. Pretot, B. Zeghmati, G. Le Palec, Theoretical and experimental study of natural convection on a horizontal plate, Appl. Thermal Eng. 20 (2000) 873–891.
[4] I. Sezai, A.A. Mohamad, Natural convection from a discrete heat source on the bottom of a horizontal enclosure, Int. J. Heat Mass Transfer 43 (2000) 2257–2266.
[5] R.F. Boehm, D. Kamyab, Analysis of established natural convection due to stripwise heating on a horizontal surface, ASME J. Heat Transfer 99 (1977) 294.
[6] T.Y. Chu, C.E. Hickox, Thermal convection with large viscosity variation in an enclosure with localized heating, ASME J. Heat Transfer 112 (1990) 388–395.
[7] O. Aydin, W.J. Yang, Natural convection in enclosures with localized heating from below and symmetrical cooling from sides, Int. J. Numer. Meth. Heat Fluid Flow 10 (2000) 518–529.
[8] N. Katsavos, I. Pappa, I. Lekakis, I.E. Sarris, N.S. Vlachos, Study of Natural convection from a heating line source of a high Prandtl number fluid in a rectangular cavity, Fifth World Conference on Experimental Heat Transfer, Fluid Dynamics and Thermodynamics, Thessaloniki, Greece, 2001, pp. 591–596.
[9] A.F. Emery, J.W. Lee, The effects of property variations on natural convection in a square enclosure, ASME J. Heat Transfer 121 (1999) 57–61.
[10] E. Plumat, Development and prospectives of furnaces for glass melting, J. Non-Cryst. Solids 26 (1977) 179–261.
[11] I.E. Sarris, I. Lekakis, N.S. Vlachos, Glass melt recirculation controlled by a heated strip in the tank bottom, Proceedings of the First Balkan Conference on Glass, Volos, Greece, 2000, pp. 379–388.
[12] K.-B. Cheong, K.-M. Moon, T.-H. Song, Treatment of radiative transfer in glass melts: validity of Rosseland and $P-1$ approximations, Phys. Chem. Glasses 40 (1999) 26–33.
[13] A. Moult, Two- and three-dimensional mathematical models of glass tank furnaces, Glass Technol. 23 (1982) 106–112.
[14] A. Oberbeck, Uber die Warmeleitung der Flussigkeiten bei Berucksichtigung der Stromungen infolge von Temperaturdifferenzen, Ann. Phys. Chem. 7 (1879) 271–292.
[15] J. Boussinesq, Theorie analytique de la chaleur, Gauthier-Villars, Paris, 2, 1903.
[16] O.R. Hofmann, Boussinesq approximation to compute the temperature and velocity distribution in glass melts, Glastechish Bericte 65 (1992) 239–245.
[17] W. Jian, Z. Zhihao, Investigation into glass tank geometries by means of a mathematical model, Glastechish Bericte 65 (1992) 1–8.
[18] S.V. Patankar, D.B. Spalding, A calculation procedure for heat, mass and momentum transfer in three-dimensional parabolic flows, Int. J. Heat Mass Transfer 15 (1972) 1787–1806.
[19] B.P. Leonard, A stable and accurate convective modelling procedure based on quadratic upstream interpolation, Comput. Meth. Appl. Mech. Eng. 19 (1979) 59–98.
[20] T. Hayase, J.A.C. Humphrey, R. Greif, A consistently formulated QUICK scheme for fast and stable convergence using finite-volume iterative calculation procedure, J. Comput. Phys. 98 (1992) 108–118.
[21] I.E. Sarris, Numerical simulation of heat and mass transfer in industrial glass-melting tanks, PhD thesis, University of Thessaly, Volos, Greece, 2001.
[22] Vahl G. De Davis, Natural convection of air in a square cavity: A bench mark numerical solution, Int. J. Numer. Meth. Fluids 3 (1983) 249–264.
[23] M.M. Canzarolli, L.F. Milanez, Natural convection in rectangular enclosures heated from below and symmetrically cooled from the sides, Int. J. Heat Mass Transfer 38 (1995) 1063–1073.
[24] K.O. Lim, K.S. Lee, T.H. Song, Primary and secondary instabilities in a glass-melting surface, Numer. Heat Transfer 36 (1999) 309–325.
[25] A. Bejan, Convection Heat Transfer, John Wiley, New York, 1984.
[26] D. Poulikakos, Natural convection in a confined fluid-filled space driven by a single vertical wall with warm and cold regions, ASME J. Heat Transfer 107 (1985) 867–876.
[27] R.J. Goldstein, K.-S. Lau, Laminar natural convection from a horizontal plate and the influence of plate-edge extensions, J. Fluid Mech. 129 (1983) 55–75.
[28] Z. Rotem, L. Claassen, Natural convection above unconfined horizontal surfaces, J. Fluid Mech. 38 (1969) 173–192.
[29] W.M. Lewandowski, Natural convection heat transfer from plates of finite dimensions, Int. J. Heat Mass Transfer 34 (1991) 875–885.
[30] L. Pera, B. Gebhart, Natural convection boundary layer flow over horizontal and slightly inclined surfaces, Int. J. Heat Mass Transfer 16 (1973) 1131–1146.
[31] T.S. Chen, H.C. Tien, B.F. Armaly, Natural convection on horizontal, inclined, and vertical plates with variable surface temperature or heat flux, Int. J. Heat Mass Transfer 29 (1986) 1465–1478.
[32] W. Muschick, A. Muysenberg, Round robin for glass tank models, Glass Sci. Technol. 71 (1998) 153–156.